Lead-free perovskite and double perovskite solar cells

Lead-free perovskite and double perovskite solar cells.

Aqel Mashot Jafar[1], Kawther A. Khalaph[2] and Amar Moula Hmood[3]

[1]Solar Energy Research Center, Renewable Energy Directorate, Higher Education and Scientific Research Ministry/ Baghdad/ Iraq.

[2]Medical College, Ibn Sina University of Medical and Pharmaceutical Sciences, Baghdad, Iraq.

[3]Materials Researches Directorate, Higher Education and Scientific Research Ministry, Baghdad, Iraq

1. aqeel@scbaghdad.edu.iq, 2. Kawthar.ali1104a@csw.uobaghdad.edu.iq, 3.dr.amarmoula@scbaghdad.edu.iq.

Abstract. The toxicity and instability of lead- halide perovskite materials in the solar cells are yet demands must be resolved to vie to find alternatives of free lead-based halide perovskites and double perovskite materials. Here we report on the experimental synthesis of a new family of lead-free inorganic halide double perovskites Cesium copper antimony chloride ($Cs_2CuSbCl_6$) and perovskite Cesium copper chloride (CsCuCl3) as a based sensitizer of the solar cells and studies of its characterize and optical properties of the Photo-Voltaic (PV) device. The configuration structural of PV devices is (FTO/TiO_2/$CsCuCl_3$ or $Cs_2CuSbCl_6$/Cu_2O/Al electrode). The double perovskite $Cs_2CuSbCl_6$ and Perovskite $CsCuCl_3$ are successfully synthesized, performed of structural investigations by X-ray diffraction, and depicted of optical properties via optical absorption of UV−vis measurement. The perovskite ($CsCuCl_3$) belongs to the space grope P6122 and the Hexagonal structure phase. The strongest peeks of the XRD diffraction pattern of the double perovskite $Cs_2CuSbCl_6$ are taken at the reflection points (-201), (-202), (-3-11), (220), (-223) and (-5-34). From UV−vis measurements obtained values of a direct gap of both ($Cs_2CuSbCl_6$) and ($CsCuCl_3$) are (1.5 and 2.2) eV, respectively. The optimum power conversion efficiency (PCE) of the PV device which used $Cs_2CuSbCl_6$ as a sensitizer is 0.94%, the filling factor is 24%, the open-circuit voltage is 582.5 mV and the short circuit current was 2.656 mA. The measurement is carried out under one sun intensity illumination (1000 W/m^2).

Key Words: Perovskite, Double Perovskite, Free-Lead.

1. Introduction

Free- Lead Perovskite of inorganic halides materials with a chemical formulas, ABX_3 and A_2BCX_6, where A represents a monovalent non-organic molecule, B and C are metal of a positive valence group, and X are an halogen anions [1]. These materials have recently attracted of a tremendous amount of interest in the solar cells society. The free lead perovskite solar cells based on

this materials are stilled under investigation and research [2]. Previous studies refer that major part of materials in this family have a stabilization phase anti decomposition and exhibit flexible synthesis of optical properties with gaps in the range from infrared to ultraviolet radiation. These unique features, coupled with low cost solutions, make them an ideal candidate as new generation optical absorbers [3]. In previous literature, efforts has been made by researchers to understand how structural Characteristics and optical properties affect the performance of photovoltaic (PV) devices [4] ,[5]. The structure and synthesis of the photovoltaic thin films were investigated by analysis X-ray diffraction (XRD). The morphology of the surface was studied by EDAX electron microscope [6]. The spectral analysis of the thin films in solar cell, the energy band gap and range energy bands of HOMO, LUMO were studied [4], [7].Here, in the current work, the Free-Lead perovskite materials such as $CsCuCl_3$ and double perovskite materials as $Cs_2CuSbCl_6$ were investigated as absorption layer in the perovskite photo-voltaic devices, which were not previously studied according to the researcher's survey of the literature studies as absorption layer in photovoltaic device. We try to investigate the performance of this materials as the thin film for absorption or harvesting the light in the photovoltaic device of perovskite solar cells. In addition, the studying investigates of the structural characteristics and optical properties of this material.

2. Basic theory :

The perovskite material CsCuCl3 have a direct optical band gap[6] . The allowed direct transition of optical band gap was expressed accordance to the equation (1) [8].

$$\boldsymbol{hv * \alpha = B * [hv - E_g]^{1/2}} \ldots . (\mathbf{1})$$

Where, ν is the light frequency, h is the Planck constant, Eg is the optical energy gap, B is empirical constant and (α) is the absorption coefficient which expressed as the equation (2) according to the Beer-Lambert law for optical absorption of the thin film [9].

$$\boldsymbol{\alpha = 2.303 \frac{A}{t}} \ldots \ldots (\mathbf{2})$$

Where A is the Absorbance of a film which have thickness (t), The relation between the Extinction Coefficient (ko) and the Absorption coefficient (α) is shown in the equation (3) :

$$\boldsymbol{K_o = \alpha * \lambda / 4\pi} \ldots . (\mathbf{3})$$

Where λ is expressed the wave length of the incident light . The relation between the Refractive Index N_o and the Extinction Coefficient K_o is expressed in the equation (4) :

$$\boldsymbol{N_o = \left[\frac{4R}{(R-1)^2} - K_o^2\right]^{1/2} - \frac{(R+1)}{(R-1)}} \ldots \ldots (\mathbf{4})$$

Where the R is the reflectance of the film. The relations between the Extinction Coefficient (K_o) with the Real and the Imaginary of the Dialectic Constants (C_r and C_I) as shown in the equations 5 and 6[10], respectively [10].

$$\boldsymbol{C_R = N_O^2 - K_O^2} \ldots \ldots (\mathbf{5})$$

$$\boldsymbol{C_I = 2 * K_O * N_O} \ldots \ldots . . (\mathbf{6})$$

Where the No is represented to the refractive index. The Power Conversion Energy (PCE) and Full Factor (F.F.) of a solar cell are calculated by using equations (7) and (8) [11] ,[12], [13]:

$$\boldsymbol{PCE = \frac{V_{0c} \cdot I_{SC} \cdot FF}{P_{in} * A_{SC}}} \ldots \ldots (\mathbf{7})$$

$$\boldsymbol{F.F. = \frac{I_m V_m}{I_{sc} V_{oc}} = \frac{P_m}{I_{sc} V_{oc}}} \ldots \ldots \ldots (\mathbf{8})$$

Where, (V_{OC}), (I_{SC}), (I_m) , (V_m) and (A_{sc}) are the open circuit voltage, short circuit current, Maximum current, Maximum Voltage and active area of the solar cell, respectively. The power conversion efficiency (PCE) can be improved by increasing the photo-generated current (I_{ph}) which correlated of the Quantum Efficiency (QE) of PV device. QE is defines that the number of charge

carrier collected of the solar cell divided on the number of incident photons while I_{ph} only takes into account the absorbed photons. QE expresses with the following formula [14] :

$$\boldsymbol{Q.E.} = \frac{\boldsymbol{h} * \boldsymbol{C}}{\boldsymbol{q} * \boldsymbol{\lambda}} * \frac{\boldsymbol{I_{ph}}}{\boldsymbol{P_{in}}} \ldots\ldots\ldots (\mathbf{9})$$

where *c* is the light speed, *h* is Planck's constant, *q* is the electronic charge, λ is the wavelength, and P_{in} is the power incident on the PV device.

3. Characterization of samples:

Crystal structure and composition studied via X- Ray Diffraction using (XRD Shimadzu 6000, Cu-Kα) for coating film sample. The surface morphology of sample and the formations of the perovskite crystals studied via the Scanning Electron Microscope (SEM) (Bruker Nano GmbH, Germany). Light I-V Measurements are recorded as the Test Reports via the Photovoltaic measurements system which composed of Oriel I−V test station and an Oriel Solar simulator. The solar simulator is type AAA for spectral performance which have uniformity of irradiance, and temporal stability. A xenon lamp with a power 450 W equipped the solar simulator. The output power is adjusted to match (1000 W m^{-2}). I−V curves are calculated via a computer which connected with an external bias to the PV cell and measuring Iph with a Keithley model 2400 digital source meter. The transmittance and absorption of film coated are analyzed via (SPECTRO UV/Vis Double Beam (UVD-3500) Labomed ,Inc) in the wavelength range of (190 - 1200) nm. The temperature of the substrates of deposition processes is monitored via an infrared temperature indicator in the any run of the experimental. Quantum Efficiency measurement system contains of monochromatic at (300-900)nm, reflector halogen lamp (75)W, and Kethley to record I_{ph}.

4. Experimental:

4.1. *Materials and solvents:*

Copper chloride $CuCl_2$ (99%) and cesium chloride CsCl (99%) were purchased from Fluka AG. Glass substrates of Fluorine-doped Tin Oxide (FTO) was employed as electrodes Transparent Conductive Oxide (TCO) which purchased of Visiontek, sheet Resistance 8 Ω/□ at dimensions (2x2) cm^2. Dioxide Titanium TiO_2 (99%) nano-particles> 30 nm of powder was origin of China. Copper oxide Cu_2O (99%) was purchased from BDH. N,N Di Methyl Formamide (DMF) (99.9% anhydrous) was purchased from Sigma Aldrich. Hydrochloric acid HCl (35.4%) was purchased from Fluka Chemika.

4.2. Preparation of Perovskite precursor solution:

The cesium copper chloride Perovskite precursor solution was synthesized by dissolving 0.134 g (1 mmol) of copper chloride ($CuCl_2$) in 2.0 ml of hydrochloric acid at room temperature and completed to 10 ml via adding DMF to obtain the sample A. Following by, 0.168 g (1 mmol) of cesium chloride was dissolved in 3 ml of hydrochloric acid at room temperature and completed to 10 ml via adding DMF to obtain the sample B. After complete dissolution of the materials as precursors solutions, two samples, A and B, were mixed in the Becker on the starrier and increased the temperature at 70°C with 30 minutes time [6].

precursor solution of double perovskite Cs2CuSbCl6 was prepared of the reaction of the $SbCl_3$ (228 mg, 1 mmol) and $CuCl_2$ (98 mg, 1 mmol) were dissolved in 10 mL DMF. Then, CsCl (336 mg, 2 mmol) was dissolved in 2 mL of hydrochloric acid and completing to 10mL by adding DMF, following by adding the Cs precursor solution to the previously made solution of Sb and Cu of salts precursor. Black precipitates were obtained by ultrasound sonication of the reaction mixture for 30 s to obtain $Cs_2CuSbCl_6$ precursor solution [15] , [4].

4.3. Preparation of Cu2O precursor solution:

Precursor solution of Copper oxide is prepared via dissolving 0.143g (1mmol) of Cu2O in 8ml of 1-butanol and adding 2ml of deionized water on the hot starrier at 50^{o}C temperature and 10 min time.

4.4. PV Device fabrication:

Preparation of compact layer TiO_2 of photo-electrode is a first fabricated of PV device by employment Aerosol Assisted Chemical Vapor Deposition (AACVD) technique via using Ultrasonic Atomizer (402AI) as deposition system doing with ultrasonic frequency (1.5MHz) [13],[12].The precursor solution, which preparation of Nano particles> 20 nm of TiO_2 powder dispersed via Ultra-sonically frequency in ethanol solvent ,is sprayed on per-heated FTO at 450 ^{o}C, the time of deposition is 1h. The hot substrates are left to cold at 50^{o}C. Following by, the perovskite precursor solution of $CsCuCl_3$ or $Cs_2CuSbCl_6$ are deposited by drop casting on (FTO/ TiO_2) substrates and annealing at 100^{o}C. Following by depositing Cu_2O precursor solution by drop casting process and annealing at 100^{o}C. Then, put a foil of Al with area 0.1cm^2 as a counter electrode on Cu_2O layer to obtain two samples of Free-Lead Perovskite Solar Cells (FLPSCs) with the configurations (FTO/ TiO_2/$CsCuCl_3$/Cu_2O/Al) and (FTO/ TiO_2/$Cs_2CuSbCl_6$/Cu_2O/Al) as shown in figure (1) which depicts the structure thin films of Photo-Voltaic (PV) device.

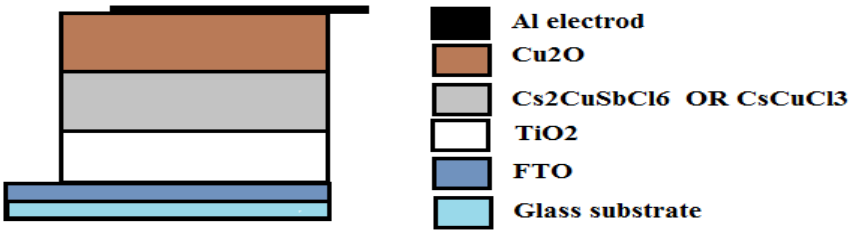

Figure (1). structure thin films of configurations FLPSCs.

5. Results and Discussion:

5.1. Structural Studies:

Figure(2-a) depicts the XRD pattern of TiO_2 thin film (Red line), which achieved by depositing of TiO_2 precursor solution via using AACVD on preheated glass substrate at 400 ^{o}C and 1 hour deposited time. The reflections are indicated to the tetragonal TiO_2. Reflections positions (black bars) of (101), (004), (204) and (301) corresponding with tetragonal structure are indicated to TiO_2 Anatase system by PDF # 211272 for comparative. Reflection position of (210) corresponding with tetragonal structure is indicated to TiO_2 Rutile system by PDF # 211276. Figure (2-b) depicts XRD pattern of the perovskite structure of $CsCuCl_3$ thin film sample which prepared via drop casting process on glass substrate followed by annealing at 100 ^{o}C. XRD pattern, red curve, of $CsCuCl_3$ perovskite is exhibited the Hexagonal structure phase, belonged the space grope P6122 and can be confirmed by PDF # 180349 at reflections positions of (100), (103), (110), (202), (204), (300) and (222). Figure (2-c) shows the patterns XRD of the thin film of $Cs_2CuSbCl_6$ depositing on glass substrate which was preparation by drop casting process Followed by annealing to 100 ^{o}C at 15 min. The XRD patterns of the sample preparation appear with red curve line in the figure (2-c), but the black bars are denoted to the double perovskite $Cs_4CuSb_2Cl_{12}$ [15]. The strongest peeks of pattern lines of the sample preparation are taken at the reflection points (-201), (-202), (-3-11), (220), (-223) and (-5-34). Figure (3-a,b) shows the high-resolution Scanning Electron Micrographs (SEM) images of thin film of CsCuCl3 and $Cs_2CuSbCl_6$, respectively, which have been deposited by drop casting process on glass substrates, followed by annealing at 100 ^{o}C temperature and 15 min deposited time. The (SEM) image clearly show the transformation from particles to aggregations structure in the sample of $CsCuCl_3$, as can be seen from these micrograph (a), but the structure of particles are nearly crystals in shape with reasonably uniform size distributions size (1- 2)μm of SEM image of $Cs_2CuSbCl_6$ sample. The scale bars of the images are 10 μm, scanning with high voltage 10kV and magnification 5 kx.

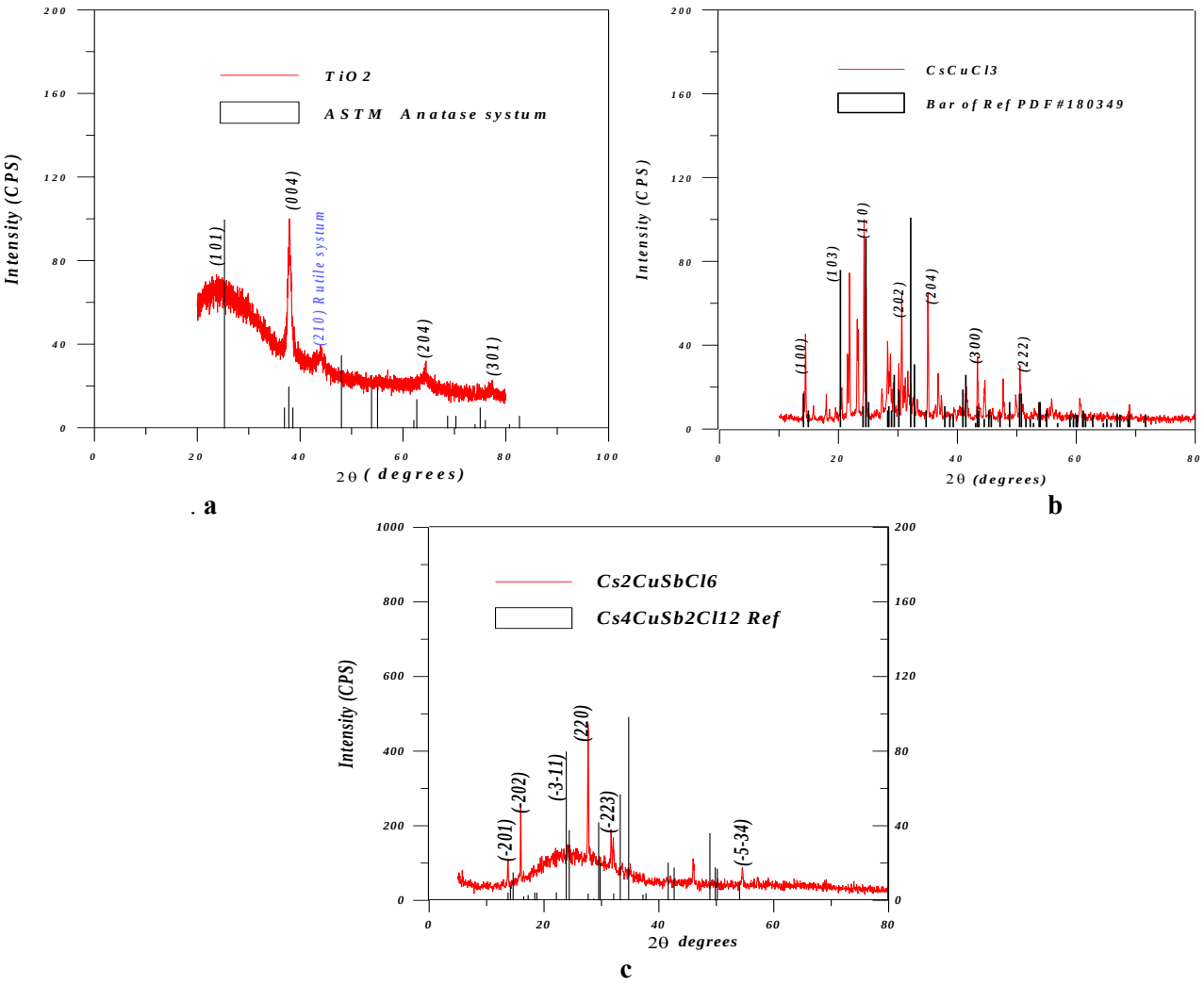

Figure (2).XRD of thin film of (a) TiO_2 (b) $CsCuCl_3$ (c) $Cs_2CuSbCl_6$.

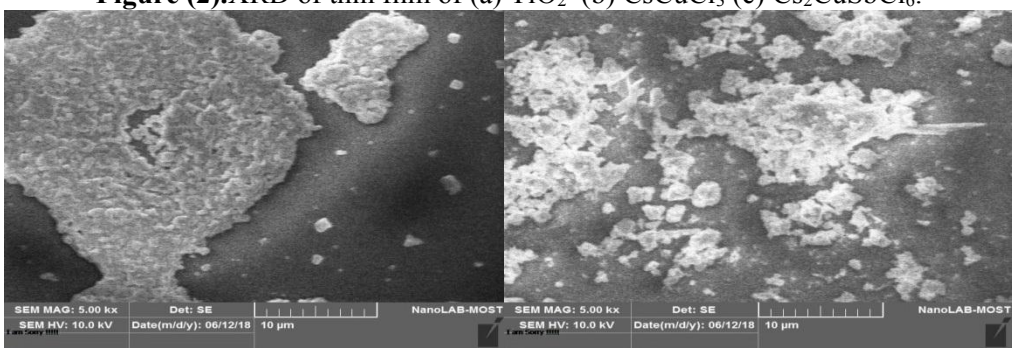

(a) **(b)**

Figure (3). Top SEM images thin film of (a)$CsCuCl_3$ (b) $Cs_2CuSbCl_6$.

5.2. Optical Studies:

Figure(4-a) is illustrated the absorbance of Pb-free halide perovskite thin films and it clears more absorbance of the sample $Cs_2CuSbCl_6$ than other sample $CsCuCl_3$. Both of the samples are analyzed at

the wavelength range (300-1100) nm employing a (UV/VIS Double Beam SPECTRO (UVD-3500) Labomed, Inc.) and blank glass substrates as the reference samples.

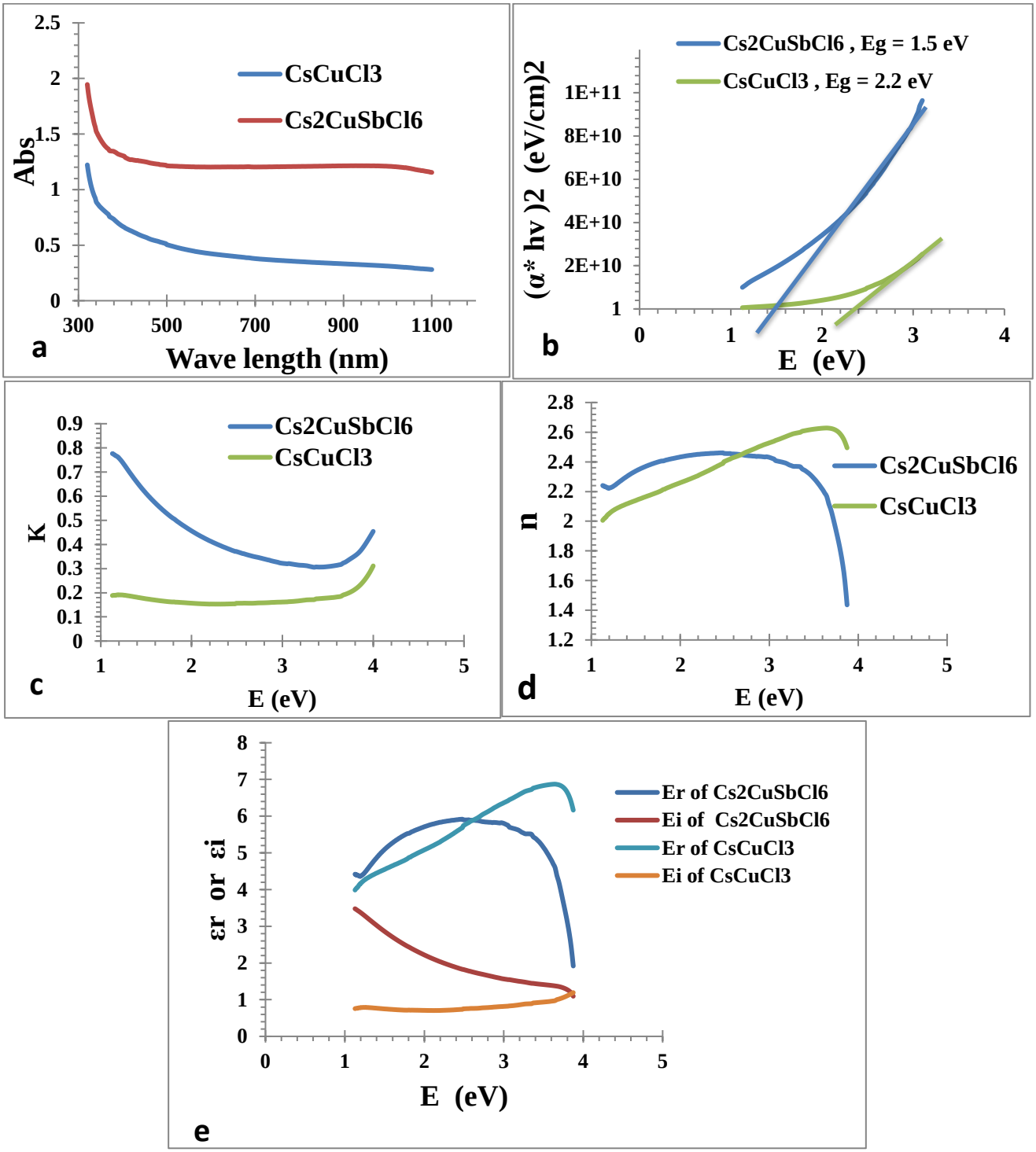

Figure (4). Optical properties of the thin film of $Cs_2CuSbCl_6$ and $CsCuCl_3$. (a) Absorbance (b)Optical Energy gap (c) extinction coefficient (d) Refractive Index and (e)Real and Imaginary parts of dielectric constant.

Plots of photon energy (hv) versus $(\alpha hv)^2$ for the thin films of deposited peroveskite materials on glass substrates are estimated of Absorption charts of the thin film which have the thickness (400nm) as shown in Figure 7(b). Pb-free halide perovskites materials $CsCuCl_3$[6], and Cs2CuSbCl6[4] have a direct optical band gap energy (E_g) which is determined of both samples by fitting the absorption data to the direct transition equation (4). The values of optical band gaps are estimated by extrapolating the linear part of the curves $(\alpha hv)^2$ as a function of the energy, E , intercept with the E axis at $\alpha = 0$. The E_g values of $CsCuCl_3$ and $Cs_2CuSbCl_6$ via data UV-Vis are estimated (2.2 and 1.5)eV which corresponding to the reported of References of [6], [4] , [16], respectively, as depicted in figure 4-b and table 1.

Figure (4-c) is depicted the extinction coefficient (k_o) to the free-lead halide perovskite films of $Cs_2CuSbCl_6$ and $CsCuCl_3$ materials. The extinction coefficient (k_o) refers to the amount of attenuation of the electromagnetic wave as it passes through the physical medium, and expresses the basis of value that determined by electromagnetic wave interactions with the medium. In figure (4-c), It can be observed clearly that the best interactions of electromagnetic wave of the visible light absorption with $Cs_2CuSbCl_6$ than other material, $CsCuCl_3$. Figure (4-d) is depicted the Refractive Index (n_o) to the free-lead halide perovskite films of $Cs_2CuSbCl_6$ and $CsCuCl_3$ materials. The refractive index (n) is a function of reflectivity (R) and extinction coefficient (K_o) as the basis of the equation (4). According of the Figure (4-d), the spectral refractive index and its energy change of the visible range were estimated about (2 to 2.6) of the $CsCuCl_3$ film but estimated (2.3 to 2.4) of the $Cs_2CuSbCl_6$ film at the visible range of the energy. Figure (4-e) depicts the real εi and imaginary εr parts of the dielectric constant as a function of the photon incident energy to the free-lead halide perovskite films of $Cs_2CuSbCl_6$ and $CsCuCl_3$ materials. The interaction between light and material charges is due to the absorption of energy in the material, and thus polarization of the medium's charges. This polarization is usually described by the dielectric constant complex (ε), Real and Imaginary parts, as shown of equations 5 and 6. The behavior of εi is similar to refractive index because the smaller value of ko^2 comparison of n^2, while εr is mainly depends on the k_o values, which are related to the variation of absorption coefficient. The imaginary part represents the absorption associated of radiation by free charges carriers [17]. The imaginary part of the dielectric constant is a measure less than of real part of dielectric constant (εr> εi), as shown in figure (4-e), the imaginary part of the dielectric constant is a measure of absorption of the energy of the radiation failing by the atoms of the material.

5.3. Performance of P.V. Devices Studies::

Figure (5) depicts the report of the measurements by the Photovoltaic measurements system of I-V curve of FLPSCs with configurations (a): (FTO/ $TiO_2/Cs_2CuSbCl_6/Cu_2O$/Al) and (b): (FTO/ $TiO_2/CsCuCl_3/Cu_2O$/Al). The measurement is carried out under intensity illumination (1000 W/m^2), active area of solar cell is 0.4 cm^2 and sweeping voltages in the scan-direction with a scan rate of s = 50 mV/s. Figure (5-a) is illustrated I-V curves of photovoltaic device that employs of $Cs_2CuSbCl_6$ as absorption layer and have the best efficiency of performance FLPSCs, (PCE = 0.94%). All the parameters of the performance FLPSCs are inserted in the table (1). The best efficiency is achieved to the FLPSC which have $Cs_2CuSbCl_6$ as a sensitizer due to the best optical properties, higher absorption and lower optical energy gap, than other sensitizer or absorption layer $CsCuCl_3$, as shown in figure (5) and table (1). R_s and R_{sh} in the table (1) are expressed the reverse slop of the (I-V) curve at points V_{oc} and I_{sc}, respectively, and determined the F.F. values [18]. It can to be observed the small values of F.F. of the solar cells (F.F.=24%), due to the low values of R_s and high values of R_{sh} of PV devices as shown in table (1). The PV devices which have typical F.F. must to be have very low value of R_s and very high value of R_{sh}.

Table 1. Performances parameters of FLPSCs have active area (0.4cm^2).

FLPSCs	E_g(eV)	V_{oc}(mV)	I_{sh}(mA)	V_m(mV)	I_m(mA)	P_m(μW)	FF	E_{ff}%	R_s(Ω)	R_{sh}(Ω)
$Cs_2CuSbCl_6$	1.5	582.5	2.656	302.0	1.241	374.95	0.24	0.94	147.8	787.95
$CsCuCl_3$	2.2	361.7	1.790	196.4	0.787	154.57	0.24	0.39	341.8	862.92

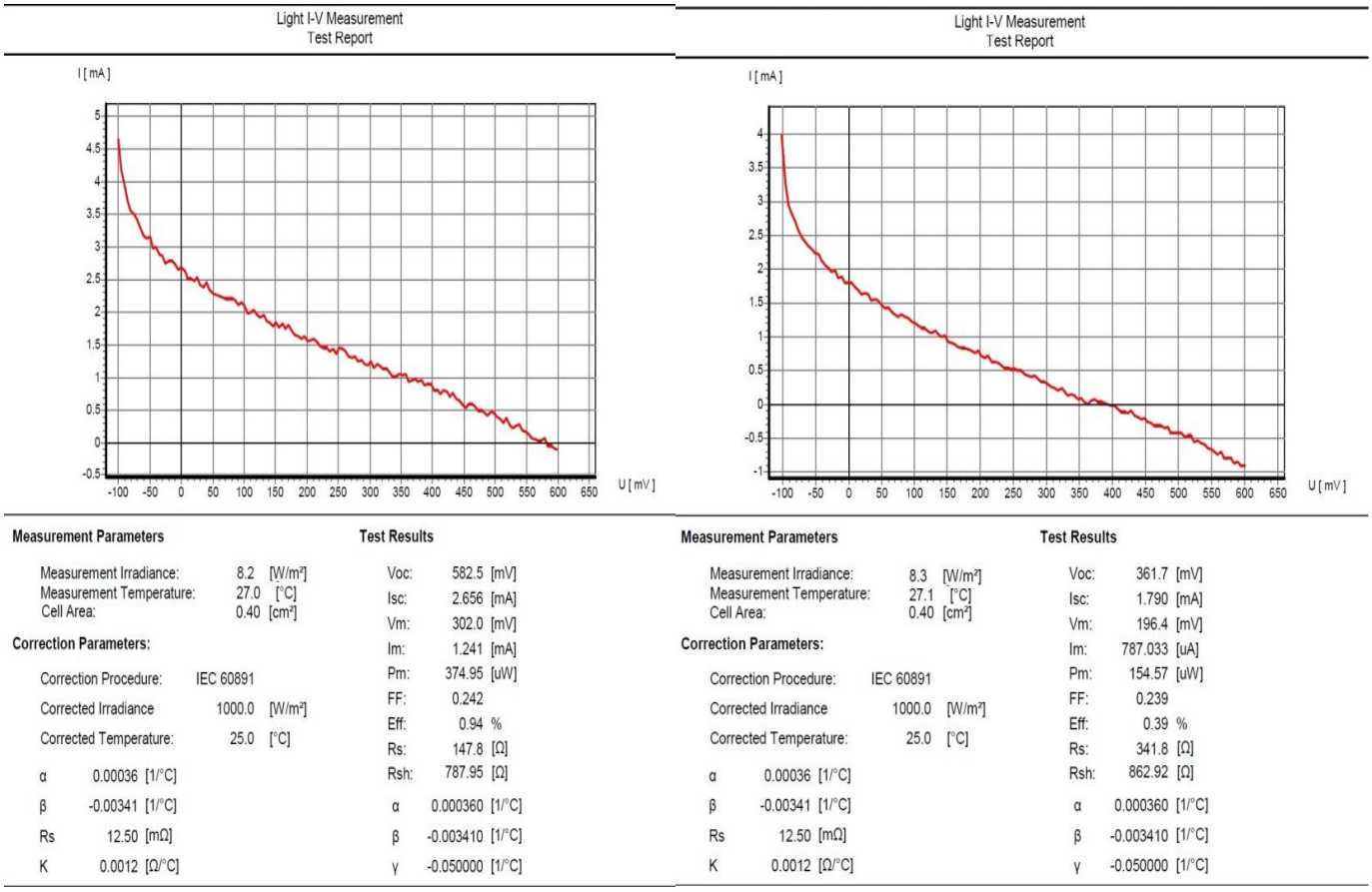

(a) ***(b)***

Figure 5. I-V curve of FLPSCs have (a): $Cs_2CuSbCl_6$ and (b): $CsCuCl_3$ as absorption of PV device.

The data of the Quantum Efficiency (Q.E.) in the wave length range (300-900)nm is recorded by Quantum Efficiency measurement system which contains of monochromatic at (300-900)nm, reflector halogen lamp (75)W, and Kethley to record Iph , as shown in figure (6-a). The output light power of the reflector halogen lamp at the wavelength range (300-900)nm, input power (P_{in}) of the solar cell sample, is calculated via employing power solar meter and monochromatic as shown in figure (6-b).

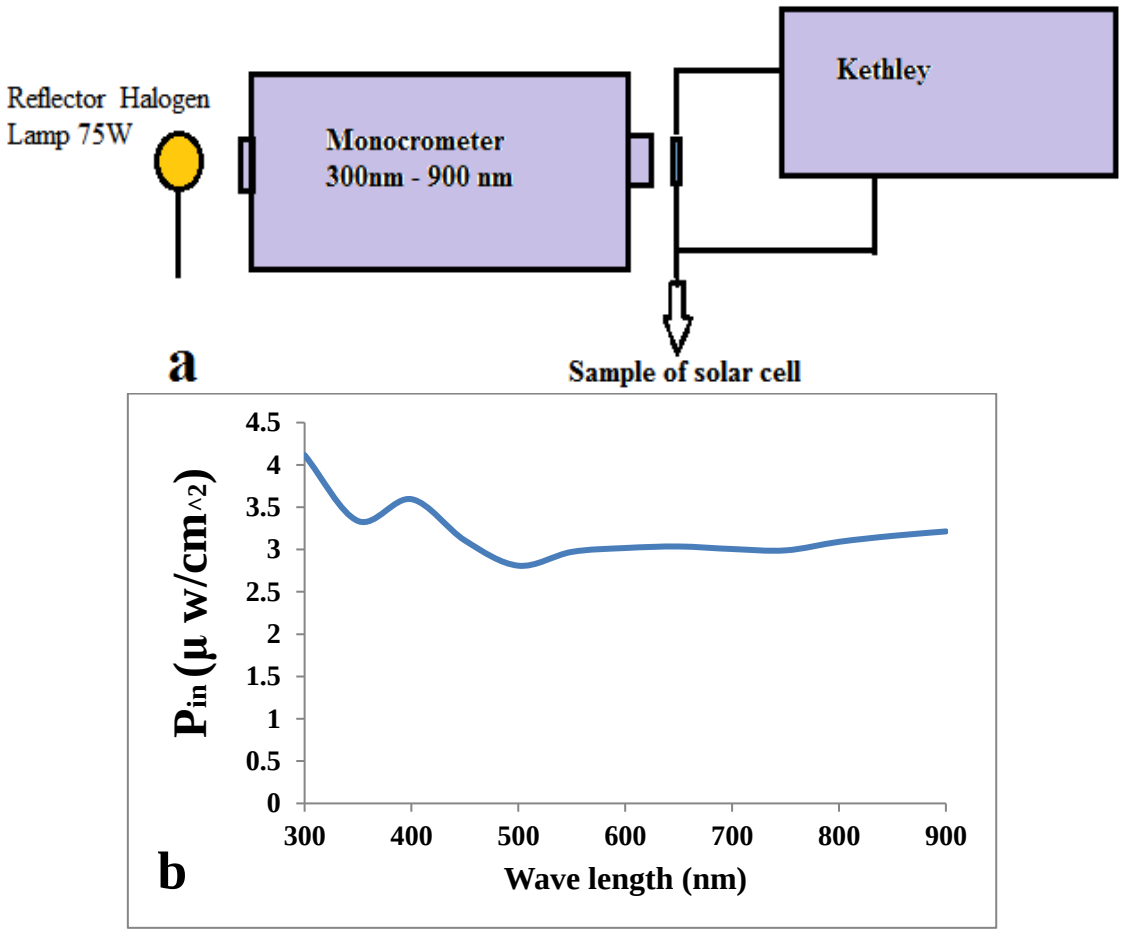

Figure 6. depicts (a): Quantum Efficiency measurement system and (b): Input power on PV device at wave length range (300-900)nm.

Figure (7) depicts the (Q.E.) of the PV device with configurations (a): (FTO/ TiO_2/$Cs_2CuSbCl_6$/Cu_2O/Al) and (b): (FTO/ TiO_2/$CsCuCl_3$/Cu_2O/Al). It is clearly visible in Figure (7-a) that the Q.E. is observed to be increased with wavelength in the range of 350-750 nm. It is reached to maximum at wave length 500 nm, beyond this maximum decreased rapidly and found minimum at the wavelengths 300 nm and 900 nm. The decreasing rapidly of the Q.E. curve of peak at wave length 500nm is observed that may be attributed to the decreased rapidly of behavior in the absorption curve as shown in figure (7-a). The increased of the Q.E. curve at the visible range (300-900) in figure (7-a) confirms the increased efficiency of the PV device that have $Cs_2CuSbCl_6$ as sensitizer, comparative with the other PV device as shown in figure (5). It is clearly of the Figure (7-b) that the Q.E. curve of PV device which have CsCuCl3 as sensitizer is observed to be decreased gradually with increased the wavelength in the range of 350-750 nm. It is reached to maximum Q.E. at 300 nm, decreased gradually and found minimum Q.E. at the wavelengths 650 nm. This behavior of Q.E. curve is similar to absorption curve of the $CsCuCl_3$ sensitizer as shown in figure (7-b).

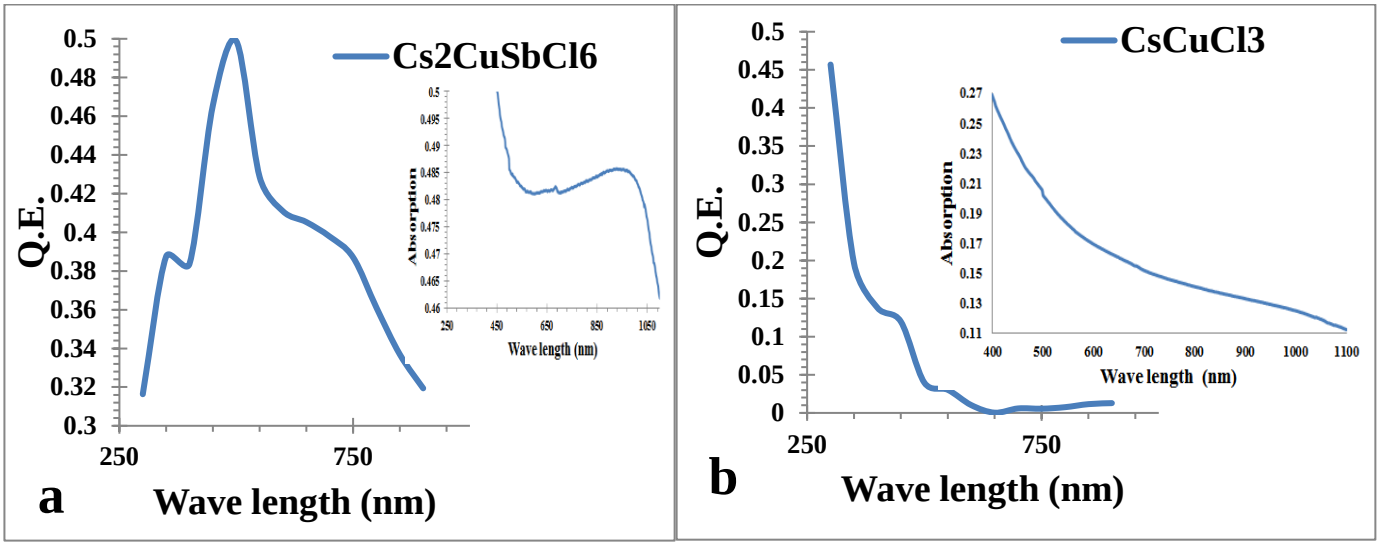

Figure 7. depicts Q,E. at wave length range (300-900)nm of PV device have (a): Cs2CuSbCl6 (b): CsCuCl3 as sensitizer.

6. Conclusion :

In summary, through a combined studies of optical and structural properties of a new family of free-lead halide double-perovskite, we have observed that its correlated of the P.V. devices performance. Perovskite $CsCuCl_3$ and double perovskite $Cs_2CuSbCl_6$ were successfully synthesized and then, FLPSCs with construction structural (FTO/TiO_2/ $Cs_2CuSbCl_6$ OR $CsCuCl_3$ /Cu_2O/Al electrode) have been successfully fabricated. The empirical results give that an optimum PCE = 0.94 % can be achieved by using double pereovskite, $Cs_2CuSbCl_6$, as harvesting light layer in FLPSC, while PV device which have $CsCuCl_3$ as a sensitizer is given (PCE= 0.39%) . It is attributed that the PCE of PV device was correlated with the absorption curve of sensitizer material and the quantum efficiency curve of PV device Performances of the wave length spectrum. The optical characterization of the double perovskite $Cs_2CuSbCl_6$ and perovskite $CsCuCl_3$ indicating a direct gap semiconductor.

7. Acknowledgements :

The authors would like to thank Ministry of Science and Technology, Renewable Energy Directorate, Baghdad-Iraq, and Materials Research Directorate, Baghdad-Iraq, for their support in the present work.

References

[1] F. Giustino and H. J. Snaith, “Toward Lead-Free Perovskite Solar Cells,” *ACS Energy Lett.*, vol. 1, no. November, p. 1233–1240, 2016.

[2] S. F. Hoefler and G. Trimmel, “Progress on lead-free metal halide perovskites for photovoltaic applications : a review,” *Monatshefte für Chemie - Chem. Mon.*, vol. 148, no. 5, pp. 795–826, 2017.

[3] A. Jain, O. Voznyy, and E. H. Sargent, “High-Throughput Screening of Lead-Free Perovskite-like Materials for Optoelectronic Applications,” 2017.

[4] Brenda Vargas, E. Ramos, E. Pérez-Gutiérrez, J. C. Alonso, and and D. Solis-Ibarra, “A Direct

Bandgap Copper−Antimony Halide Perovskite," *J. Am. Chem. Soc.*, no. 139, p. 9116−9119, 2017.

[5] Xingang Zhao *et al.*, "Design of Lead-Free Inorganic Halide Perovskites for Solar Cells via Cation-Transmutation," *J. Am. Chem. Soc.*, vol. 139, no. 7, pp. 2630–2638, 2017.

[6] Muhammad Aamir, "SYNTHESIS OF METAL HALIDE PEROVSKITE MATERIALS FOR LIGHT HARVESTING APPLICATIONS," Allama Iqbal Open University, Islamabad, 2018.

[7] P. Karuppuswamy *et al.*, "Role of a hydrophobic scaffold in controlling the crystallization of methylammonium antimony iodide for efficient lead-free perovskite solar cells," *Nano Energy*, vol. 45, no. December 2017, pp. 330–336, 2018.

[8] A. M. Jafar, K. Al-amara, T. M. Lafta, M. H. Mahmod, and I. M. Abood, "Fabrication and Characterization of P-Type Co-Doped Tin Oxide Nano-Films," *Elixir Int. J.*, vol. 65, no. June 2013, pp. 19799–19803, 2013.

[9] A. M. Jafar, K. Al-Amara, F. L. Rashid, and A. I. K. Fayyadh, "Fabrication and Characterization of Fluorine-Doped Tin Oxide Transparent Conductive Nano-Films," *Int. J. Innov. Res. Eng. Sci.*, vol. 6, no. 2, pp. 49–58, 2013.

[10] M. N. Al-Jabery, Q. A. Abbas, and Hamid S. Al-Jumaili, "Study the optical properties of CuInS 2 non stoichiometric thin films prepared by chemical spray pyrolysis method," *Iraqi J. Phys.*, vol. 10, no. 19, pp. 70–75, 2012.

[11] A. M. Jafar, M. H. Suhail, and Falah I. Mustafa, "Organolead Iodide Perovskite Solar Cells (OPSC)," *AASCIT J. Energy*, vol. 2, no. 6, pp. 81–87, 2016.

[12] M. H. Suhail and A. M. Jafar, "Fabrication and Characterization of Organolead Halide Peroviske Solar Cell," *Elixir Int. J.*, vol. 98, no. September 2016, pp. 42709–42713, 2016.

[13] A. M. Jafar, M. H. Suhail, F. M. Al-Attar, and and M. K. Kalaf, "ORGANOLEAD HALIDE PEROVSKITE SOLAR CELLS," in *32st European Photovoltaic Solar Energy Conference and Exhibition*, 2016, pp. 1296–1302.

[14] S. Chander, A. Purohit, A. Nehra, S. P. Nehra, and M. S. Dhaka, "A Study on Spectral Response and External Quantum Efficiency of Mono-Crystalline Silicon Solar Cell," vol. 5, no. 1, pp. 1–4, 2015.

[15] N. Singhal, R. Chakraborty, P. Ghosh, and A. Nag, "Low-Bandgap Cs 4 CuSb 2 Cl 12 Layered Double Perovskite : Synthesis , Reversible Thermal Changes , and Magnetic Interaction," pp. 2085–2092, 2018.

[16] G. Volonakis *et al.*, "Lead-Free Halide Double Perovskites via Heterovalent Substitution of Noble Metals," 2016.

[17] C. Kittel and H. Y. Fan, *Introduction to Solid State Physics Eighth Edition*. 2005.

[18] G. Sissoko and S. Mbodji, "A Method to Determine the Solar Cell Resistances from Single IV Characteristic Curve Considering the Junction Recombination Velocity (Sf)," *International Journal of Pure and Applied Sciences and Technology*, vol. 6, no. 2. pp. 103–114, 2011.